THE JOURNAL OF PHYSICAL CHEMISTRY B

Article

Cite This: J. Phys. Chem. B 2019, 123, 4527−4533

pubs.acs.org/JPCB

Positively Charged Tags Impede Protein Mobility in Cells as Quantified by ^{19}F NMR

Yansheng Ye,[†,§] Qiong Wu,[†,§] Wenwen Zheng,[†] Bin Jiang,[†] Gary J. Pielak,[‡] Maili Liu,[†] and Conggang Li*[,†]

[†]Key Laboratory of Magnetic Resonance in Biological Systems, State Key Laboratory of Magnetic Resonance and Atomic and Molecular Physics, National Center for Magnetic Resonance in Wuhan, Wuhan National Laboratory for Optoelectronics, Wuhan Institute of Physics and Mathematics, Chinese Academy of Sciences, Wuhan 430071, China

[‡]Department of Chemistry, Department of Biochemistry and Biophysics, Integrative Program for Biological and Genome Sciences, and Lineberger Comprehensive Cancer Center, University of North Carolina at Chapel Hill, Chapel Hill, North Carolina 27599, United States

ABSTRACT: Proteins are often tagged for visualization or delivery in the "sea" of other macromolecules in cells but how tags affect protein mobility remains poorly understood. Here, we employ in-cell ^{19}F NMR to quantify the mobility of proteins with charged tags in *Escherichia coli* cells and *Xenopus laevis* oocytes. We find that the transient charge−charge interactions between the tag and cellular components affect protein mobility. More specifically, positively charged tags impede protein mobility.

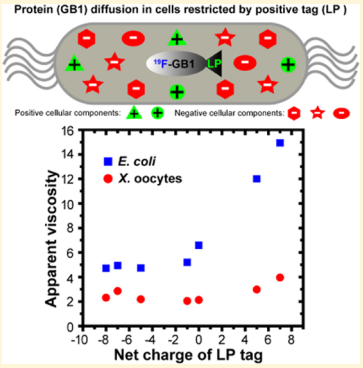

INTRODUCTION

Protein mobility is critical for cellular function. The cellular environment, which contains up to 500 g/L of macromolecules, affects protein diffusion,[1,2] mainly via transient and weak "quinary" interactions such as electrostatic attraction between the test protein and other cellular components.[3−6] Proteins are often tagged in biochemistry and biotechnology. For example, cell-penetrating peptide (CPP) tags are used to deliver proteins into cells.[7,8] Green fluorescent protein (GFP) tags are used to assess protein diffusion in cells.[9] Lanthanide-binding peptide tags are used as luminescent probes for protein interaction studies[10] and to measure residual dipolar couplings and paramagnetic effects in NMR studies.[11,12] Do tags affect the cellular diffusion of test proteins?

A tag may interact with other cellular components, affecting test protein diffusion. Fluorescently tagged GFP itself takes part in nonspecific weak interactions with cellular components to slow diffusion, as demonstrated by experiments and simulations.[13−15] The so-called "inert" protein GB1 interacts with cellular components when linked to Arg-rich CPP (Tat) tags, even when the Arg motifs are short.[16,17] The effect of tags on protein mobility remains poorly understood. Here, we use in-cell ^{19}F NMR to probe the interaction between a GFP tag and other cellular components. We also use in-cell ^{19}F NMR to quantify the effects of charge−charge interactions from the lanthanide-binding tag on GB1 mobility in living cells.

EXPERIMENTAL SECTION

Constructing GB1-LP(−5) and Its Variants. The coding sequence for the lanthanide-binding peptide (LP) tag YIDTNNDGWYEGDELLA (net charge of −5) was fused to the 5′ end of the coding region of GB1. For protein expression, GB1-LP(−5) was cloned into the PET21a vector under the control of a T7 promoter. GB1-LP mutants of different net charges were obtained by site-directed mutagenesis of the LP tag and confirmed by sequencing. The details are given in Table 1.

Constructing UBQ-LP(−8). The coding sequence for the lanthanide-binding peptide (LP) tag mutant YIDEDDDGWYEGDELLA (net charge of −8) was fused to the 5′ end of the coding region for ubiquitin (UBQ). For protein expression, UBQ-LP(−8) was cloned into the PET21a vector under the control of a T7 promoter.

Constructing GFP Variants. The construction of GFP-(+36), GFP(−30), and GFP(−7) has been described in ref 18. The full length genes (synthesized by Sangon, Shanghai, China) were inserted into the plasmid pUC19. The target gene for each GFP mutant was amplified from pUC19 and inserted to a pET28a vector for expression.

Received: March 7, 2019
Revised: April 24, 2019
Published: May 1, 2019

DOI: 10.1021/acs.jpcb.9b02162
J. Phys. Chem. B 2019, 123, 4527−4533

Table 1. GB1 (Net Charge of −4) Tagged with LP (sequence after break) of Different Charges[a]

GB1-LP(−8)	MQYKLILNGKTLKGETTTEAVDAATAEKVFKQYANDNGVDGEWTYDDATKTFTVTE YIDEDDDGWYEGDELLA
GB1-LP(−7)	MQYKLILNGKTLKGETTTEAVDAATAEKVFKQYANDNGVDGEWTYDDATKTFTVTE YIDTDDDGWYEGDELLA
GB1-LP(−5)	MQYKLILNGKTLKGETTTEAVDAATAEKVFKQYANDNGVDGEWTYDDATKTFTVTE YIDTNNDGWYEGDELLA
GB1-LP(−1)	MQYKLILNGKTLKGETTTEAVDAATAEKVFKQYANDNGVDGEWTYDDATKTFTVTE YIDTNNDGWYQGKQLLA
GB1-LP(0)	MQYKLILNGKTLKGETTTEAVDAATAEKVFKQYANDNGVDGEWTYDDATKTFTVTE YINTNNNGWYQGNQLLA
GB1-LP(+5)	MQYKLILNGKTLKGETTTEAVDAATAEKVFKQYANDNGVDGEWTYDDATKTFTVTE YIKTNNKGWYKGKKLLA
GB1-LP(+7)	MQYKLILNGKTLKGETTTEAVDAATAEKVFKQYANDNGVDGEWTYDDATKTFTVTE YIKTKKKGWYKGKKLLA

[a]Net charge of LP indicated in parentheses was assessed using PROTEIN CALCULATOR v3.4 at pH 7.0.

Protein Expression and Purification. Plasmids containing genes for GB1-LP(−5) and its variants of six net charges, UBQ, UBQ-LP(−8), GFP(+36), GFP(−30), and GFP(−7) were transformed into *Escherichia coli* BL21 (DE3) cells. Cells containing GFP(+36), GFP(−30), and GFP(−7) were selected with 50 μg/mL kanamycin. The others were selected with 100 μg/mL ampicillin. The cells were grown at 37 °C with shaking at 220 rpm. The expression was induced with isopropyl β-D-thiogalactopyranoside (IPTG, final concentration, 1 mM) when the optical density at 600 nm (OD_{600}) reached 0.8−1.0. ^{15}N enrichment and 3-fluorotyrosine (3FY) labeling were achieved using $^{15}NH_4Cl$ and 3-fluorotyrosine (3FY) plus glyphosate.[13] For 5-fluorotryptophan (5FW) labeling, 60 mg of 5-fluoroindole (5FI) was added to 1 L of cell cultures when the OD_{600} reached 0.8.[19]

GB1-LP(−8), GB1-LP(−7), GB1-LP(−5), GB1-LP(−1), GB1-LP(0), and UBQ-LP(−8) were purified using a DEAE Fast Flow column (GE Healthcare) with buffer A (50 mM Tris-HCl, pH 8.0) and buffer B (50 mM Tris, 1 M NaCl, pH 8.0). The fractions were further purified by size-exclusion chromatography (HiLoad Superdex75 16 mm/600 mm column, GE Healthcare) using buffer C (50 mM Tris, 250 mM NaCl, pH 8.0). GB1-LP(+5) and GB1-LP(+7) were purified using an SP Fast Flow column (GE Healthcare) with buffer D (50 mM sodium acetate, pH 5.0) and buffer E (50 mM sodium acetate, 1 M NaCl, pH 5.0). The fractions were further purified by size-exclusion chromatography (HiLoad Superdex75 16 mm/600 mm column) using buffer F (50 mM sodium acetate, 250 mM NaCl, pH 5.0). UBQ and UBQ-LP(−8) were purified as described.[20]

GFP(+36), GFP(−30), and GFP(−7) were purified using a HisTrap Ni−NTA affinity column with buffer G (50 mM Tris, 2 M NaCl, 10 mM imidazole, pH 8.0) and buffer H (50 mM Tris, 2 M NaCl, 500 mM imidazole, pH 8.0) and further purified by size-exclusion chromatography (HiLoad Superdex75 16/600 column) using buffer C (50 mM Tris, 250 mM NaCl, pH 8.0).

Sample Preparation for *E. coli* NMR. Generally, after 2 h of IPTG induction at 37 °C, the cell cultures (usually ∼150 mL) were harvested by centrifugation at 2000*g* for 10 min at room temperature. The cell pellets were gently resuspended in 0.5 mL of M9 buffer (6.5 g/L Na_2HPO_4, 3.0 g/L, KH_2PO_4, and 1.0 g/L NaCl) containing 10% D_2O and transferred to a 5 mm NMR tube. For GFP(+36), GFP(−30), and GFP(−7), 200 mL of cell culture was harvested after IPTG induction for 20 h at 25 °C. Supernatants were collected immediately after each NMR experiment by centrifugation (2000*g*, 10 min) to assess leakage.[21] No leakage was observed.

Sample Preparation for *Xenopus* Oocyte NMR. *Xenopus* oocytes were prepared as described in ref 22, 23. Healthy-looking, stage-VI oocytes were chosen manually and stored in ND96 (96 mM NaCl, 2 mM KCl, 1.8 mM $CaCl_2$, 1 mM $MgCl_2$, 5 mM HEPES, pH 7.4) buffer containing 10 μg/mL ampicillin and streptomycin at 18 °C and used within 1 week. Microinjection was conducted as described in refs23, 24. Generally, each oocyte was injected with ∼20 nL of ∼5 mM purified proteins using a IM-300 microinjector (Narishige Co. Ltd., Tokyo, Japan). The injected oocytes (150 or more) were put into a Shigemi NMR tube containing ND96 buffer plus 10% D_2O. After in-cell NMR, 200 μL of buffer above the oocytes was used to assess leakage. No leakage was observed.

Sample Preparation for *in Vitro* NMR. *E. coli* cells containing ^{15}N-enriched, 5FW-labeled GB1-LP(+7) from 150 mL of culture were pelleted and resuspended in 0.5 mL of lysis buffer (20 mM KH_2PO_4, 50 mM NaCl, pH 6.5). The suspensions were sonicated on ice for 20 min with a duty cycle of 3 s on and 6 s off. The clear lysates obtained after centrifugation (16 000*g*, 30 min) were used for NMR. For NaCl titration experiments, the cell lysis buffer used is 20 mM KH_2PO_4, pH 6.5, and NaCl of 4 M stock solution was added into the clear lysates with final concentrations of 50, 100, 200, and 500 mM. RNase and DNase, at a final concentration of 1 mg/mL, were added into the clear lysates separately. Then, 100 mM $MgCl_2$ were introduced into the clear lysates with or without RNase and DNase. *E. coli* genomic DNA was extracted using a TIANamp Bacteria DNA kit (TIANGENBIOTECH (BEIJING) Co., Ltd.) and added into the protein sample (0.125 mM in 20 mM KH_2PO_4, 50 mM NaCl, pH 6.5) with a protein/DNA ratio of 1:1 (w/w). The *E. coli* membrane was prepared as described in ref 23 and added into the protein sample (0.25 mM in 20 mM KH_2PO_4, 50 mM NaCl, pH 6.5) with a protein/lipid ratio of 1:1 (w/w).

NMR Experiments. One-dimensional ^{19}F spectra of the test proteins in several glycerol/H_2O solutions (0, 24, 36, and 48% w/w), in *E. coli* cells, and in *Xenopus* oocytes were acquired, and ^{19}F relaxation times for 5FW-labeled GB1 and its mutants were measured. Data were acquired at 22 °C on a Bruker 600 MHz spectrometer equipped with an H/F/(C, N) triple resonance cryogenic probe. The acquisition time for ^{19}F experiments was generally less than 2 h. The sweep widths were 12 kHz, and up to 2048 scans were collected with a duty cycle delay of 2 s. The acquisition time was 0.73 s. For GFP and its variants in cells, up to 8192 scans were collected for ^{19}F experiments, which required less than 6.5 h. T_1 was measured by inversion recovery. T_2 was measured with a CPMG sequence.[25,26] The acquisition time for relaxation experiments was less than 5 h. In general, the sweep width was 6 kHz, and up to 384 scans were collected with a duty cycle delay of 2−4 s. The acquisition time was 0.73 s. $^{15}N-^{1}H$ HSQC spectra were acquired at an ^{1}H frequency of 599.81 MHz with an ^{1}H spectral width of 9578.544 Hz and an ^{15}N spectral width of 2431.420 Hz. The matrix size was 2048 by 256. The acquisition times were 52.6 ms (t_1) and 107.0 ms (t_2). Typically, 16 scans per complex t_1 increments were

DOI: 10.1021/acs.jpcb.9b02162
J. Phys. Chem. B 2019, 123, 4527−4533

accumulated for a total measurement time of ~1.5 h. The bacterial viability (assessed by colony plating)[27] for the in-cell samples after 6 h of NMR is 90 ± 10%. In-cell NMR samples were tested for leakage after data collection. No leakage was observed. ^{19}F chemical shifts were referenced to trifluorotoluene at −63.72 ppm. Data were processed with Topspin 2.1 or 3.1 software.

RESULTS

First, we assessed interaction of the GFP tag and its charge variants with the intracellular environment of *E. coli* and *Xenopus laevis* oocytes by ^{19}F NMR. GFP and its variants were labeled with 5-fluorotryptophan (5FW) at their sole tryptophan at position 67. Labeling was achieved using 5-fluoroindole.[19] In buffer, the ^{19}F linewidths of variants with net charges of −30, −7, and +36 are similar, except for GFP −30, which seems to have two conformations (Figure 1). ^{19}F

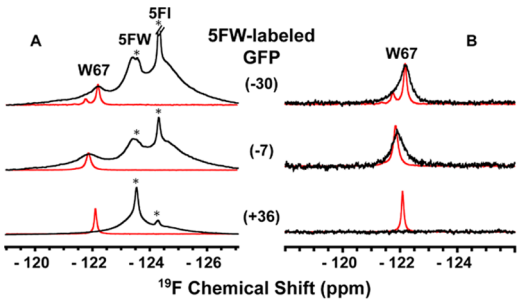

Figure 1. ^{19}F spectra of 5FW-labeled GFP variants with different net charges (−30, −7, and +36) in *E. coli* cells (A, black), *Xenopus* oocytes (B, black) and buffer (red). Resonances from free 5-fluoroindole (5FI) and 5-fluorotrptophan (5FW) are marked by asterisks.

resonances are broadened in cells compared to buffer. The effect is most extreme for GFP with a net charge of +36 in that its spectrum is completely absent in *E. coli* and oocytes (Figure 1). We attribute this broadening to the nonspecific weak interactions between GFP and other cellular components.[13−15] This observation shows that the positively charged GFP variant is involved in strong interactions with macromolecules in cells, consistent with the report that positively charged GFP mainly interacts with negatively charged ribosomes.[28]

To further investigate charge effects, the inert protein GB1 was tagged at its C terminus with the lanthanide-binding peptide (LP) or its variants with charges from −8 to +7, resulting in protein net charges ranging from −12 to +3 (Table 1). We maintained the size of the constructs to avoid size effects.[15,29] The constructs were labeled, and ^{19}F spectra were acquired in cells (Figure 2). We observe two peaks for each construct. The peak at a lower field is from W43 of GB1. The other peak is from the tag. Two additional signals are observed in *E. coli*, one each from free 5FW and 5-fluoroindole (FI).[25] In *E. coli*, the linewidth of the protein signal broadens as the net positive charge of the tag increases, especially for constructs with positively charged tags. In oocytes, this phenomenon is less obvious. The broadening may be due to the interactions between the positively charged tag and negatively charged cellular components.

To confirm the charge−charge interaction between the test protein and cellular components, we collected 1D ^{19}F and ^{15}N−^{1}H HSQC NMR spectra of ^{15}N-enriched, 5FW-labeled GB1-LP (+7, net charge of LP) in fresh *E. coli* lysates at

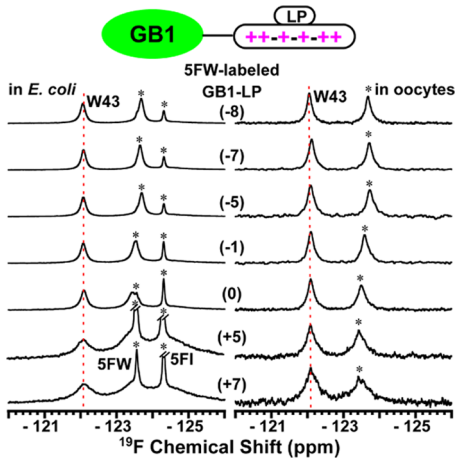

Figure 2. ^{19}F spectra of 5FW-labeled GB1-LP with different charges (in parentheses) in *E. coli* cells and oocytes. Asterisks indicate resonances from free 5FW, 5FI, and the labeled tryptophan residue from the tag, which is overlapped with 5FW in *E. coli*.

different salt concentrations (Figure 3). ^{19}F linewidths for W43 from the target protein are narrower upon increasing the NaCl concentration (Figure 3, left panel), suggesting that the broadening is attributable to charge−charge interactions between the test protein, especially the positively charged LP tag, and other cellular components. ^{15}N−^{1}H HSQC spectra also showed that more signals were observed with increasing salt concentration, consistent with the ^{19}F result.

To understand the charge effect, we quantified the tag charge dependence of protein rotational mobility in cells by measuring ^{19}F relaxation for each GB1-LP construct (Figure 4).[25] ^{19}F longitudinal relaxation (T_1) measurements on 5-fluorotryptophan-labeled proteins have been used to assess protein rotational mobility in living cells by assuming that the proteins tumble as spheres and the label is rigid.[30] Therefore, the ^{19}F resonance from W43, but not the one from the flexible tag, where the internal correlation time may dominate T_1,[25] was selected for analysis. The T_1 data show that GB1 linked to LP with different charges tumble similarly in *E. coli* with an intracellular viscosity of two to three times that of water and in oocytes with a viscosity one to two times that of water (Figure 4A), consistent with a previous study.[26]

Transverse relaxation rates (R_2) are sensitive to protein interactions.[25] The viscosity obtained from R_2 is attributable to the sum of the real intracellular viscosity and the effect of weak protein interactions. Thus, R_2 provides an alternative approach to assess weak protein interactions in cells.[25] The viscosities derived from R_2 in *E. coli* are around five times those of water, and the values are independent of the net charges of negatively charged LPs (Figure 4B). When the LP tag has no net charge, the test protein experiences an apparent viscosity of approximately seven times that of water, which is almost the same as that experienced by GB1 without the tag.[25] When GB1 is tagged with a positively charged LP, the apparent intracellular viscosity increases with net positive charge (Figure 4B). This phenomenon is more marked in *E. coli* than in oocytes, indicating that the same positively charged tag is involved in more or stronger nonspecific attractive interactions in *E. coli*. In summary, the effect of charge−charge interactions between the tag and other cellular components can be quantified using ^{19}F NMR, and proteins with positively

DOI: 10.1021/acs.jpcb.9b02162
J. Phys. Chem. B 2019, 123, 4527−4533

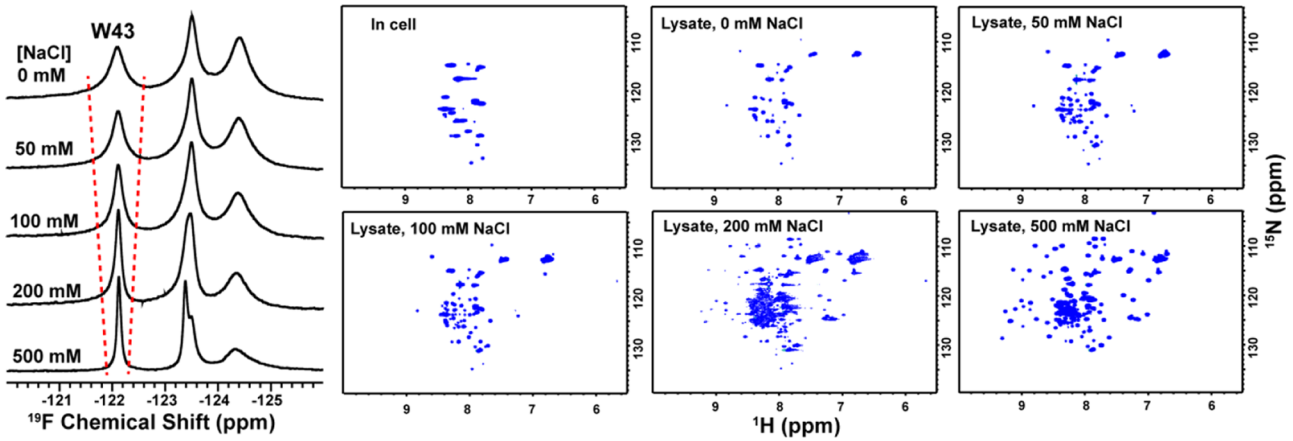

Figure 3. ^{19}F (left panel) and ^{15}N−^{1}H HSQC (right panel) spectra of ^{15}N-enriched, 5FW-labeled GB1-LP(+7) in cell lysates at different NaCl concentrations. The in-cell ^{15}N−^{1}H HSQC (right panel) spectrum is also shown. The W43 resonance is indicated.

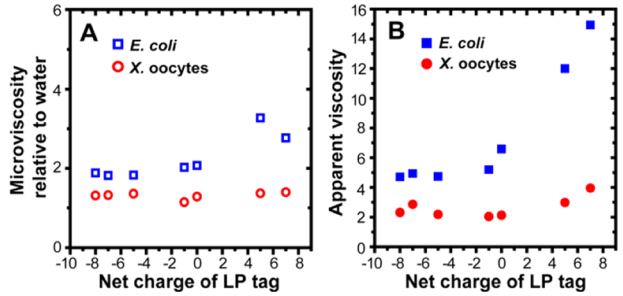

Figure 4. Dependence of cellular viscosity probed by GB1-LP on the net charge of the LP tag. (A) Microviscosity in *E. coli* cells and in *Xenopus* oocytes calculated from T_1 data is shown as blue squares and red circles, respectively. (B) Apparent viscosities in *E. coli* and *Xenopus* oocytes calculated from R_2 data are shown as solid squares and circles, respectively.

charged tags experience more or stronger transient interactions in cells.

To confirm this conclusion, ubiquitin (UBQ, no net charge at physiological pH) was linked to a negatively charged LP (net charge −8) and labeled with 3-fluorotyrosine (3FY).The width of ^{19}F resonance from Y59 of UBQ-LP(−8) in *E. coli* is less than that of wild-type UBQ in *E. coli* (Figure 5). This result implies that we can utilize a small negatively charged tag to reduce quinary interaction and thereby enhance the sensitivity and resolution of in-cell spectra. This behavior in oocytes, however, is less obvious, probably because there are fewer macromolecules interacting with UBQ.[26,31]

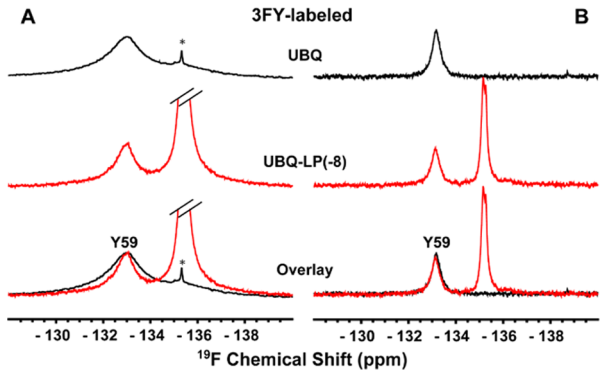

Figure 5. ^{19}F spectra of 3FY-labeled UBQ (black) and UBQ-LP (red, LP net charge of −8) in living *E. coli* cells (A) and *Xenopus* oocytes (B). Asterisks indicate the resonance from free 3-fluorotyrosine (3FY). The Y59 resonance is indicated.

DISCUSSION

Over past decade, small tags, CPPs for example, have been developed to deliver cargoes including nanoparticles, liposomes, nucleic acids, and proteins into cells.[32] Most CPPs are positively charged to ensure attractive interactions with the negatively charged cell membrane.[33] The proteins linked to CPPs, however, are concentrated inside endocytic organelles.[34,35] Our results using GFP-tagged- and LP-tagged-variants with positive charges demonstrate that positively charged tags are involved in more transient interactions with other cellular components and consequently impede the mobility of the tag itself and the test protein in cells.

The resolution of protein NMR, as reflected by linewidth, depends on rotational mobility. In cells, protein rotational mobility is determined by the size of the protein, its environmental viscosity, and its interactions with other components.[25] Although GB1 (6.5 kDa) gives a high-resolution in-cell spectrum, ubiquitin, a protein of similar size (8.5 kDa) does not because it is involved with more and stronger nonspecific interactions. In fact, ubiquitin is almost invisible in cells.[25,36] Reducing these weak interactions is required to obtain high quality in-cell spectra. Charge-inverting mutations have been introduced to reduce cellular quinary interactions.[2,3] Our observations on GFP variants support this conclusion. However, this approach may perturb the structure of the test protein affecting its function. Here, we suggest another approach, attaching a small tag to the end of a test protein. Such a tag is expected to be less perturbing than an amino acid change within the protein.

We first systematically quantified the effect of small LP tags with charges ranging from −8 to +7 on test protein mobility. Negatively charged tags reduce the nonspecific interactions in cells. This conclusion is further confirmed by our observations on ubiquitin (Figure 5).

Charge−charge interactions are ubiquitous in the complex cellular environment. According to the proteome isoelectric-point (pI) database,[37] 62% of the K12 *E. coli* proteome (2690 of 4314 proteins) comprises proteins with pI values less than 6.8, whereas 33% have pI values greater than 7.4. For the *Xenopus tropicalis* proteome, 55% (13 026 of 23 598 proteins)

DOI: 10.1021/acs.jpcb.9b02162
J. Phys. Chem. B 2019, 123, 4527−4533

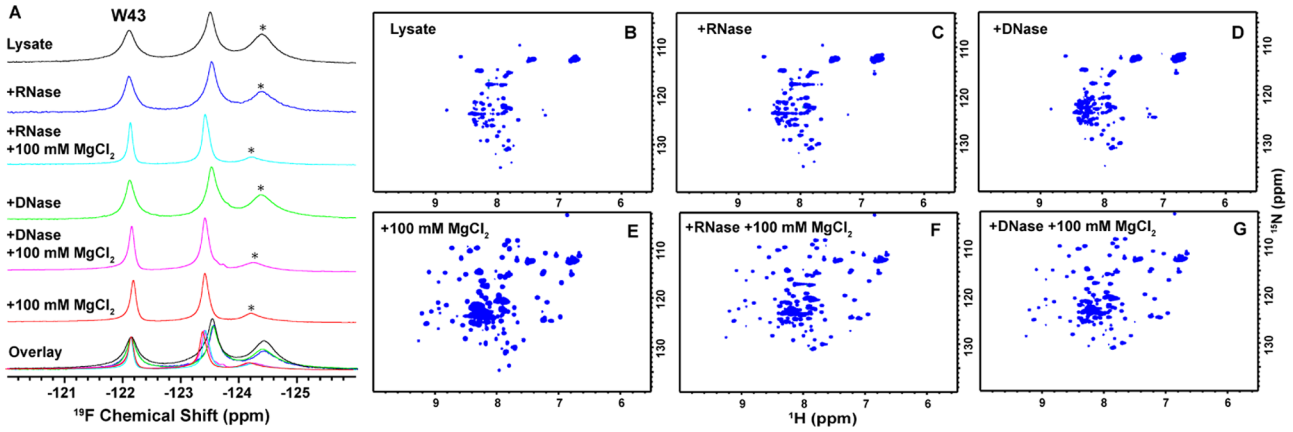

Figure 6. ^{19}F (left panel) and ^{15}N−^{1}H HSQC (right panel) spectra of ^{15}N-enriched, 5FW-labeled GB1-LP(+7) in cell lysates (A, black; B) and lysates with added RNase (A, blue; C), RNase with 100 mM $MgCl_2$ (A, cyan; F), DNase (A, green; D), DNase with 100 mM $MgCl_2$ (A, magenta; G), or 100 mM $MgCl_2$ (A, red; E). The W43 resonance is indicated. Asterisk indicates the resonance from free 5FI.

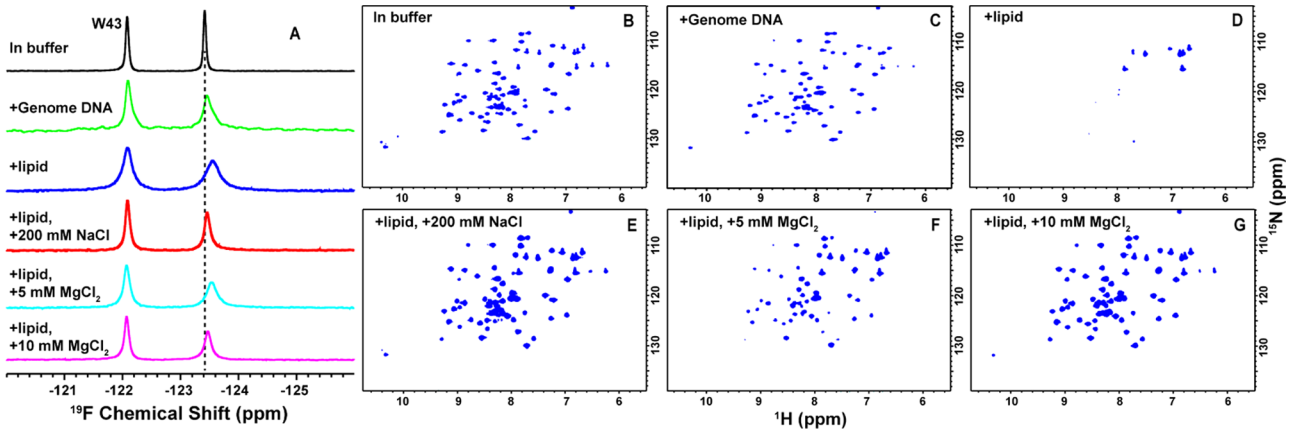

Figure 7. ^{19}F (left panel) and ^{15}N−^{1}H HSQC (right panel) spectra of purified ^{15}N-enriched, 5FW-labeled GB1-LP(+7) in buffer (A, black; B) and buffer added with genomic DNA (A, green; C) and liposome from *E.coli* membrane extract (A, blue; D, protein/lipid = 1:1, w/w), followed by the addition of 200 mM NaCl (A, red; E) or 5 mM (A, cyan; F) and 10 mM $MgCl_2$ (A, magenta; G). The W43 resonance is indicated. The dashed line indicates the resonance position from the LP tag in buffer.

possesses pI values less than 6.8, whereas 32% possesses values greater than 7.4. In summary, near physiological pH (7.4−7.8 for *E. coli* and 7.2 for the eukaryotic cytosol),[31] a majority of proteins have a net negative charge, and there is a larger percentage of proteins with a net negative charge in *E. coli* relative to oocytes. Even though some high-abundance proteins such as those associated with ribosomes are positively charged, they are highly organized and bound to RNA and the assembly has a net negative charge.[28,38] That is, proteins linked with a positively charged tag will take part in more charge−charge interactions, and this phenomenon will be more prevalent in *E. coli* compared to *Xenopus* oocytes. In addition, the higher tolerance of oocytes to charge could be due to the lower g/L concentration of macromolecules in eukaryotes.[31] These ideas are consistent with our observations on the rotational mobility of GB1-LP, ubiquitin, and GFP variants in cells.

Quinary interactions comprise both protein−protein and protein−RNA interactions.[39] We also collected 1D ^{19}F and ^{15}N−^{1}H HSQC NMR spectra of ^{15}N-enriched, 5FW-labeled GB1-LP (+7, net charge of LP) in fresh *E. coli* lysates (Figure 6). ^{19}F linewidths do not change significantly after mixing the sample with RNase or DNase, and HSQC spectra also show only a few increased signals in the disordered region but not the structured region (Figure 6C,D), suggesting that protein−RNA/DNA interactions may not be the main cause of broadening. Upon adding RNase (DNase) together with $MgCl_2$, ^{19}F linewidths decreased (Figure 6A, cyan and magenta) and signals from the structured part were detected (Figure 6F,G). However, adding $MgCl_2$ alone has a similar effect, suggesting that $MgCl_2$ also decreased the charge−charge interactions, just like NaCl (Figure 6A, red; Figure 6E). Our further experiments (Figure 7A (green) and Figure 7C) showed that the spectra for GB1-LP(+7) with and without *E. coli* genomic DNA in buffer are almost the same, indicating that the broadening effect from DNA is small.

The negatively charged membrane is another possible interaction component. We then used *E. coli* total membrane extracts to test its effect. The ^{19}F resonance is severely broadened (Figure 7A, blue), and most signals disappeared in the HSQC spectrum (Figure 7D). ^{19}F resonance sharpened (Figure 7A, red) and backbone signals reappeared upon adding NaCl (Figure 7E), indicating that charge−charge interactions between the positive tag and negative membrane components also play a key role in the broadening effect. We further tested the potential effect of $MgCl_2$ on the interaction between the protein and lipids. As observed after addition of NaCl, ^{19}F resonance became sharper (Figure 7A, cyan and magenta) and

DOI: 10.1021/acs.jpcb.9b02162
J. Phys. Chem. B 2019, 123, 4527−4533

backbone signals reappeared (Figure 7F,G) after introducing a low concentration of $MgCl_2$.

These results imply that protein−lipid and potential protein−protein interactions, but not protein−nucleic acid interactions, play a significant role in quinary interactions involving the LP tags used here. Such tags are used to produce pseudocontact shifts,[40] but this application is limited to *in vitro* studies because we find that LP tags do not specifically bind lanthanides in cells because no pseudocontact shifts are observed (data not shown). This absence may be caused by competitive binding of other ions and charge−charge interactions of the type described here.

CONCLUSIONS

We have characterized the potential interaction between a fluorescent tag, GFP, and other cellular components and systematically quantified the effects of charge−charge interactions from a small engineering tag on the GB1 mobility in living cells using ^{19}F NMR. The work provides an explanation for the effect of tags on target protein mobility under physiological conditions. We conclude that positively charged tags impede protein mobility in cells. This conclusion has implications for drug delivery and in-cell protein NMR.

AUTHOR INFORMATION

Corresponding Author

*E-mail: conggangli@wipm.ac.cn.

ORCID

Gary J. Pielak: 0000-0001-6307-542X

Conggang Li: 0000-0002-5798-1722

Author Contributions

§Y.Y. and Q.W. contributed equally to this work.

Notes

The authors declare no competing financial interest.

ACKNOWLEDGMENTS

This work was supported by the Ministry of Science and Technology of China (2017YFA0505400), the 1000 Young Talents Program, the National Natural Science Foundation of China (21575156, 21173258 and 21221064), the K.C. Wong Education Foundation to C.L., the U.S. National Science Foundation (1607359 and 14108540), and the U.S. National Institutes of Health (R01GM127291) to G.J.P.

ABBREVIATIONS

NMR, nuclear magnetic resonance; GFP, green fluorescent protein; LP, lanthanide-binding peptide; GB1, immunoglobulin-binding domain B1 of streptococcal protein G; UBQ, ubiquitin; 5FW, 5-fluorotryptophan; 5FI, 5-fluoroindole; 3FY, 3-fluorotyrosine; IPTG, isopropyl β-D-thiogalactopyranoside; CPP, cell-penetrating peptide

REFERENCES

(1) Wang, Y. Q.; Li, C. G.; Pielak, G. J. Effects of Proteins on Protein Diffusion. *J. Am. Chem. Soc.* **2010**, *132*, 9392−9397.

(2) Mu, X.; Choi, S.; Lang, L.; Mowray, D.; Dokholyan, N. V.; Danielsson, J.; Oliveberg, M. Physicochemical Code for Quinary Protein Interactions in *Escherichia coli*. *Proc. Natl. Acad. Sci. U.S.A.* **2017**, *114*, E4556−E4563.

(3) Crowley, P. B.; Chow, E.; Papkovskaia, T. Protein Interactions in the *Escherichia coli* Cytosol: An Impediment to In-Cell NMR Spectroscopy. *ChemBioChem* **2011**, *12*, 1043−1048.

(4) Cohen, R. D.; Guseman, A. J.; Pielak, G. J. Intracellular pH Modulates Quinary Structure. *Protein Sci.* **2015**, *24*, 1748−1755.

(5) Guseman, A. J.; Speer, S. L.; Goncalves, G. M. P.; Pielak, G. J. Surface Charge Modulates Protein-Protein Interactions in Physiologically Relevant Environments. *Biochemistry* **2018**, *57*, 1681−1684.

(6) Cohen, R. D.; Pielak, G. J. Electrostatic Contributions to Protein Quinary Structure. *J. Am. Chem. Soc.* **2016**, *138*, 13139−13142.

(7) Bolhassani, A.; Jafarzade, B. S.; Mardani, G. *In Vitro* and *in Vivo* Delivery of Therapeutic Proteins Using Cell Penetrating Peptides. *Peptides* **2017**, *87*, 50−63.

(8) Guidotti, G.; Brambilla, L.; Rossi, D. Cell-Penetrating Peptides: From Basic Research to Clinics. *Trends Pharmacol. Sci.* **2017**, *38*, 406−424.

(9) Miyawaki, A. Proteins on the Move: Insights Gained from Fluorescent Protein Technologies. *Nat. Rev. Mol. Cell Biol.* **2011**, *12*, 656−668.

(10) Sculimbrene, B. R.; Imperiali, B. Lanthanide-binding Tags as Luminescent Probes for Studying Protein Interactions. *J. Am. Chem. Soc.* **2006**, *128*, 7346−7352.

(11) Su, X. C.; McAndrew, K.; Huber, T.; Otting, G. Lanthanide-Binding Peptides for NMR Measurements of Residual Dipolar Couplings and Paramagnetic Effects from Multiple Angles. *J. Am. Chem. Soc.* **2008**, *130*, 1681−1687.

(12) Pan, B. B.; Yang, F.; Ye, Y. S.; Wu, Q.; Li, C. G.; Huber, T.; Su, X. C. 3D Structure Determination of a Protein in Living Cells Using Paramagnetic NMR Spectroscopy. *Chem. Commun.* **2016**, *52*, 10237−10240.

(13) Li, C. G.; Wang, G. F.; Wang, Y. Q.; Creager-Allen, R.; Lutz, E. A.; Scronce, H.; Slade, K. M.; Ruf, R. A. S.; Mehl, R. A.; Pielak, G. J. Protein ^{19}F NMR in *Escherichia coli*. *J. Am. Chem. Soc.* **2010**, *132*, 321−327.

(14) McGuffee, S. R.; Elcock, A. H. Diffusion, Crowding & Protein Stability in a Dynamic Molecular Model of the Bacterial Cytoplasm. *PLoS Comput. Biol.* **2010**, *6*, No. e1000694.

(15) Trovato, F.; Tozzini, V. Diffusion within the Cytoplasm: A Mesoscale Model of Interacting Macromolecules. *Biophys. J.* **2014**, *107*, 2579−2591.

(16) Kyne, C.; Ruhle, B.; Gautier, V. W.; Crowley, P. B. Specific Ion Effects on Macromolecular Interactions in *Escherichia coli* Extracts. *Protein Sci.* **2015**, *24*, 310−318.

(17) Kyne, C.; Crowley, P. B. Short Arginine Motifs Drive Protein Stickiness in the *Escherichia coli* Cytoplasm. *Biochemistry* **2017**, *56*, 5026−5032.

(18) Lawrence, M. S.; Phillips, K. J.; Liu, D. R. Supercharging Proteins Can Impart Unusual Resilience. *J. Am. Chem. Soc.* **2007**, *129*, 10110−10112.

(19) Crowley, P. B.; Kyne, C.; Monteith, W. B. Simple and Inexpensive Incorporation of ^{19}F-Tryptophan for Protein NMR Spectroscopy. *Chem. Commun.* **2012**, *48*, 10681−10683.

(20) Lazar, G. A.; Desjarlais, J. R.; Handel, T. M. *De Novo* Design of The Hydrophobic Core of Ubiquitin. *Protein Sci.* **1997**, *6*, 1167−1178.

(21) Barnes, C. O.; Pielak, G. J. In-cell Protein NMR and Protein Leakage. *Proteins* **2011**, *79*, 347−351.

(22) Selenko, P.; Serber, Z.; Gade, B.; Ruderman, J.; Wagner, G. Quantitative NMR Analysis of The Protein G B1 Domain in *Xenopus laevis* Egg Extracts and Intact oocytes. *Proc. Natl. Acad. Sci. U.S.A.* **2006**, *103*, 11904−11909.

(23) Ye, Y. S.; Liu, X. L.; Xu, G. H.; Liu, M. L.; Li, C. G. Direct Observation of Ca^{2+}-Induced Calmodulin Conformational Transitions in Intact *Xenopus laevis* oocytes by ^{19}F NMR Spectroscopy. *Angew. Chem., Int. Ed.* **2015**, *54*, 5328−5330.

(24) Sakai, T.; Tochio, H.; Tenno, T.; Ito, Y.; Kokubo, T.; Hiroaki, H.; Shirakawa, M. In-cell NMR Spectroscopy of Proteins Inside *Xenopus laevis* oocytes. *J. Biomol. NMR* **2006**, *36*, 179−188.

(25) Ye, Y. S.; Liu, X. L.; Zhang, Z. T.; Wu, Q.; Jiang, B.; Jiang, L.; Zhang, X.; Liu, M. L.; Pielak, G. J.; Li, C. G. ^{19}F NMR Spectroscopy as a Probe of Cytoplasmic Viscosity and Weak Protein Interactions in Living Cells. *Chem. - Eur. J.* **2013**, *19*, 12705−12710.

DOI: 10.1021/acs.jpcb.9b02162
J. Phys. Chem. B 2019, 123, 4527−4533

(26) Ye, Y. S.; Liu, X. L.; Chen, Y. H.; Xu, G. H.; Wu, Q.; Zhang, Z. T.; Yao, C. D.; Liu, M. L.; Li, C. G. Labeling Strategy and Signal Broadening Mechanism of Protein NMR Spectroscopy in *Xenopus laevis* oocytes. *Chem. - Eur. J.* **2015**, *21*, 8686−8690.
(27) Sakakibara, D.; Sasaki, A.; Ikeya, T.; Hamatsu, J.; Hanashima, T.; Mishima, M.; Yoshimasu, M.; Hayashi, N.; Mikawa, T.; Walchli, M.; Smith, B. O.; Shirakawa, M.; Guntert, P.; Ito, Y. Protein Structure Determination in Living Cells by In-cell NMR Spectroscopy. *Nature* **2009**, *458*, 102−105.
(28) Schavemaker, P. E.; Smigiel, W. M.; Poolman, B. Ribosome Surface Properties May Impose Limits on the Nature of the Cytoplasmic Proteome. *Elife* **2017**, *6*, No. e30084.
(29) Ye, Y. S.; Wu, Q.; Zheng, W. W.; Jiang, B.; Pielak, G. J.; Liu, M. L.; Li, C. G. Quantification of Size Effect on Protein Rotational Mobility in Cells by ^{19}F NMR Spectroscopy. *Anal. Bioanal. Chem.* **2018**, *410*, 869−874.
(30) Williams, S. P.; Haggie, P. M.; Brindle, K. M. ^{19}F NMR Measurements of the Rotational Mobility of Proteins *in Vivo*. *Biophys. J.* **1997**, *72*, 490−498.
(31) Theillet, F. X.; Binolfi, A.; Frembgen-Kesner, T.; Hingorani, K.; Sarkar, M.; Kyne, C.; Li, C. G.; Crowley, P. B.; Gierasch, L.; Pielak, G. J.; Elcock, A. H.; Gershenson, A.; Selenko, P. Physicochemical Properties of Cells and Their Effects on Intrinsically Disordered Proteins (IDPs). *Chem. Rev.* **2014**, *114*, 6661−6714.
(32) Li, M.; Tao, Y.; Shu, Y. L.; LaRochelle, J. R.; Steinauer, A.; Thompson, D.; Schepartz, A.; Chen, Z. Y.; Liu, D. R. Discovery and Characterization of a Peptide That Enhances Endosomal Escape of Delivered Proteins *in Vitro* and *in Vivo*. *J. Am. Chem. Soc.* **2015**, *137*, 14084−14093.
(33) Yang, N. J.; Hinner, M. J. Getting across the Cell Membrane: An Overview for Small Molecules, Peptides, and Proteins. *Methods Mol. Biol.* **2015**, *1266*, 29−53.
(34) Allen, J. K.; Brock, D. J.; Kondow-McConaghy, H. M.; Pellois, J. P. Efficient Delivery of Macromolecules into Human Cells by Improving the Endosomal Escape Activity of Cell-Penetrating Peptides: Lessons Learned from dfTAT and its Analogs. *Biomolecules* **2018**, *8*, No. 50.
(35) Erazo-Oliveras, A.; Muthukrishnan, N.; Baker, R.; Wang, T. Y.; Pellois, J. P. Improving the Endosomal Escape of Cell-Penetrating Peptides and Their Cargos: Strategies and Challenges. *Pharmaceuticals* **2012**, *5*, 1177−1209.
(36) Wang, Q.; Zhuravleva, A.; Gierasch, L. M. Exploring Weak, Transient Protein-Protein Interactions in Crowded *in Vivo* Environments by In-Cell Nuclear Magnetic Resonance Spectroscopy. *Biochemistry* **2011**, *50*, 9225−9236.
(37) Kozlowski, L. P. Proteome-pI: Proteome Isoelectric Point Database. *Nucleic Acids Res.* **2017**, *45*, D1112−D1116.
(38) Davis, J. H.; Tan, Y. Z.; Carragher, B.; Potter, C. S.; Lyumkis, D.; Williamson, J. R. Modular Assembly of the Bacterial Large Ribosomal Subunit. *Cell* **2016**, *167*, 1610−1622.
(39) Majumder, S.; Xue, J.; DeMott, C. M.; Reverdatto, S.; Burz, D. S.; Shekhtman, A. Probing Protein Quinary Interactions by In-Cell Nuclear Magnetic Resonance Spectroscopy. *Biochemistry* **2015**, *54*, 2727−2738.
(40) Nitsche, C.; Otting, G. Pseudocontact Shifts in Biomolecular NMR Using Paramagnetic Metal Tags. *Prog. Nucl. Magn. Reson. Spectrosc.* **2017**, *98*−*99*, 20−49.

DOI: 10.1021/acs.jpcb.9b02162
J. Phys. Chem. B 2019, 123, 4527−4533